Counter-ion adsorption and electrostatic potential in sodium and choline dodecyl sulfate micelles - a molecular dynamics simulation study

Rafaela Eliasquevici[1], *Kalil Bernardino*[1]*

* kalilb@ufscar.br

1. Laboratório de Química Computacional, Departamento de Química, Universidade Federal de São Carlos, Rod. Washington Luiz S/n, 13565-905 São Carlos, Brazil

Author revised version

This manuscript was published in Journal of Molecular Modeling (https://link.springer.com/article/10.1007/s00894-024-05897-1). If you use any information of this document, please cite it as:

R. Eliasquevici, K. Bernardino, *Journal of Molecular Modeling* (2024) 30:101

A pre-print version of this manuscript before revision can be found at https://www.researchsquare.com/article/rs-3874437/v1

Context

Choline-based surfactants are interesting both from the practical point of view to obtaining environmental-friendly surfactants as well as from the theoretical side since the interactions between the choline and surfactants can help to understand self-assembly phenomena in deep eutectic solvents. Although no significant change was noticed in the micelle size and shape due to the exchange of the sodium counterion by choline in our simulations, the adsorption of the choline cation over the micelle surface is stronger than the adsorption of the sodium, which leads to a reduction of the exposed surface area of the micelle and remarkable effects over the electrostatic potential. The choline neutralizes the surface charge of the surfactant better than sodium, however, this is partially compensated by a stronger water orientation around the SDS micelle. The balance between the contributions from the surfactant, the counterion and water to the electrostatic potential leads to a complex pattern with alternate regions of positive and negative potential at the micelle/water interface which can be important to the incorporation of other charged species at the micelle surface as well as for the interaction between micelles in solution.

Methods

To evaluate the effects of the counterion substitution, micelles of sodium dodecyl sulfate (SDS) and choline dodecyl sulfate (ChDS) were studied and compared by means of molecular dynamics simulations in aqueous solution. In both cases, the simulations started from pre-assembled micelles with 60 dodecyl sulfate ions and 240 ns simulations were performed at NPT ensemble at T = 323.15 K and P = 1 bar using the Gromacs software with the OPLS-AA force field to describe dodecyl sulfate and choline, Åqvist parameters for sodium and SPC model for water molecules.

1. Introduction

Self-assembled structures play a key role in biological systems, with cellular membranes being responsible for isolating regions with different chemical compositions, controlling the entry and exit of substances in the cell and more complex phenomena like phagocytosis.[1,2] In industry and laboratories, surfactants are often used to improve the

solubility of hydrophobic compounds in water, stabilize dispersions, limit the growth of nanoparticles and as a template for the synthesis of nanoporous materials.[3,4,5] Despite being different phenomena, they share a common origin as a balance between the hydrophobic effect that results in a tendency of the aliphatic portions of the surfactant or lipid molecules to avoid contact with water by clustering together or by the adsorption at interfaces, and electrostatic and/or steric repulsions between the polar portion of the molecule which limits the growth of the self-assembled structure, avoiding a phase separation.[1,2,6]

In this work, we will focus on the effect of the counterions over the electrostatic interactions involved in the micelles formed by ionic surfactants. In those systems, the repulsion between heads with the same charge and the strong interaction between them and water molecules limits the size and also defines the cluster's shape. Considering the surfactants based on dodecyl sulfate anion, the reduction of the cation radius along a homologous series as in the alkaline metals results in a systematic increase in the critical micellar concentration (CMC), which is the smallest concentration at which the micelle formation is observed.[2] Computer simulations were used to study different effects of the substitution of the counterion in surfactant systems. Liu *et al* compared the shape, solvent accessible surface area and counterion adsorption in micelles of dodecyl sulfate with sodium and several quaternary ammonium counterions and observed different binding patterns for the ammonium cations.[7] Hantal *et al* compared the adsorption of Li^+, Na^+, K^+, Rb^+, and Cs^+ cations at decyl sulfate monolayers at air/water interface and reported an increase in the Helmholtz layer thickness with increasing the ionic radius of the cation.[8] Racktin and Pack simulated dodecyl sulfate micelles with different cations and found that the counterion binding decreases on the sequence $NH_4^+ > Li^+ > Na^+$.[9] The effect of the interaction parameters between the surfactant and the counter-ion over micelle structure, which to some extent presents similar effects of possible counterions exchanges, was studied by de Moura and Freitas[10] and by Tang *et al*.[11] The salt concentration was also showed to have significant effects over the shape and dynamics of aggregates in self-assembled systems.[12,13,14,15]

Here, we will compare the widely used surfactant sodium dodecyl sulfate (SDS) with the choline dodecyl sulfate (ChDS). The micelles formed by dodecyl sulfate are well-behaved and stable. The choline cation is not only bulkier than sodium and any other alkaline metal cation, but also presents a hydroxyl group that can form hydrogen bonds, leading to a

competition between ionic and hydrogen bonds interaction with the surfactant. From the practical point, the choline cation is also interesting since the use of organic cations tends to increase the solubility of surfactants[16] and choline is a bio-compatible cation,[17,18] which can be used to design greener surfactants.[19] In order to use choline-based surfactants, it is important to know in advance how this cation can affect the surfactant self-assembly and also the interaction between aggregates. Hence, we used molecular dynamics simulations to study the effect of substituting the sodium counterion by the choline over the micelle shape, the extension of the counterion association with the micelle, and the electrostatic potential produced by the micelle, with particular interest in its long-range behavior since that controls the interaction between charged particles before they get into contact. In previous works from our group, we investigate the electrostatic potential produced by sodium octanoate monolayers at air-water interface[20] and by a SDS micelle interacting with monolayers of the same surfactant,[21] being observed in the latter a stronger counterion adsorption at the flat monolayer than at the spherical micelle surface. Other groups also characterized the electrostatic potential produced by lipid bilayers.[22,23,24] However, to the best of our knowledge, no computer simulation work so far focused on the effects of counterions exchange over the electrostatic potential of self-assembled surfactant structures.

There is also a fast-increasing interest in the use of deep eutectic solvents (DES) in replacement of traditional solvents in synthesis and extraction operations due to properties including low toxicity, great thermal stability and negligible vapor pressure,[25,26] and choline salts are present in some of the most studied DES, like reline (choline chloride + urea)[27] and ethaline (choline chloride + ethylene glycol).[28] The micelle formation is also observed in those DES, but while the CMC of non-ionic surfactants is usually larger than in water, presumably due to a decrease in the importance of the hydrophobic effect, the opposite trend is noticed for ionic surfactants, which form larger micelles and at lower concentrations in choline-based DES and in its mixtures with water than at pure aqueous solution.[29,30,31] This behavior is attributed to a more efficient screening of the electrostatic interactions due to the high ionic strength in DES. Besides an investigation of the electrostatic interactions involved in surfactant systems in DES is beyond the scope of our present work, the comparison between the SDS and ChDS systems can give some insights into how specific interactions with choline cation may affect the micelle formation and inter-micelle interactions in choline-based DES when compared to aqueous solutions.

2. Methods

Model system. In order to verify the effects of the exchange of the counterion between sodium and choline over the structure and the electrostatic potential of the micelle, this study embraces the comparison of two systems: sodium dodecyl sulfate (SDS) micelle in water (1) and choline dodecyl sulfate (ChDS) micelle in water (2). The initial structure of the N=60 micelles was made using the Packmol software[32] with the surfactant heads pointed outward from a sphere with a radius of 1.4 nm, and the terminal methyl groups remained inside a sphere with a radius of 0.85 nm. Subsequently, 42,000 solvent molecules and 60 counter-ions, sodium for system 1 and choline for system 2, were added, filling a cubic box with an edge of 16 nm. After equilibration, the volume of the simulation boxes reaches an average value of 1294.4 nm³ for SDS and 1304.7 nm³ for ChDS, resulting in molar concentrations of *ca.* 0.08 mol/L.

Simulations Conditions and Parameters. All of the simulations were performed using the GROMACS suite[33,34] (version 2021.4) with an integration step of 0.8 fs and a total time of 240 ns. An energy minimization was performed with the Steepest descent algorithm. The structural relaxation was determined by the convergence of the density of the system and the counterion adsorption over the micelle surface. All the simulations were performed in the NPT ensemble with the temperature coupled with the V-rescale algorithm,[35] with the bath temperature equal to 323.15 K and the coupling constant equal to 0.1 ps. A temperature larger than the room temperature was chosen to enable the comparison with ongoing simulations of our group with micelles in choline-based deep eutectic solvents, which are being done at 323.15 K to mitigate the slow dynamics resulting from the higher viscosity of those systems, which are orders of magnitude higher than water at room temperature but decreases significantly with the temperature.[36] The isotropic Berendsen pressure coupling[37] was used with the P = 1.0 bar and coupling constant equal to 1.0 ps. Periodic boundary conditions were used in all directions. The potential energy for dodecyl sulfate and choline ions was described using the OPLS-AA parameters[38] with the partial charges of the dodecyl sulfate head group and the first CH_2 group attached to it recalculated based on RHF/6-311G* calculations of the ethyl-sulfate anion using the geodesic method implemented in Firefly 7.1.0.[39,40] The charges

of the remaining of surfactant aliphatic tail as well as for the choline cation were taken from OPLS-AA forcefield. The torsion potentials for the H-O-C-C and O-C-C-N dihedral angles of choline cation were taken from reparametrizations performed in previous works[41] based on flexible scans performed using B3LYP-D3(BJ)/Def2-TZVPD calculations performed with Orca 4.0.0.2 software.[42] Flexible SPC model[43] was employed for water molecules and the Åqvist parameters[44] for sodium cations. Those parameters are given in the supporting information file of this manuscript (Table S1 and S5). Nonbonded interactions were truncated at 1.2 nm, with the particle-mesh Ewald correction (PME)[45] for the long-range Coulomb interactions and a shift function for the Lennard-Jones interactions starting from 1.0 nm. VMD (version 1.9.4)[46] was used to visualize the trajectories and render the graphical representations of the systems.

3. Results and Discussions

3.1 Micelle shape and counterion adsorption

Starting from pre-assembled N=60 dodecyl sulfate micelles, no surfactant dissociation was observed in the system with sodium counterions (SDS), and only one dissociation was observed in the system with choline cations (ChDS), resulting in a micelle with an aggregation number of 59 (graphical representations of the structures in Figure 1). Since only one surfactant dissociation was observed across the two systems in the 240 ns simulations, this event can be considered a rare one and cannot be used to infer anything about the differences in the thermodynamic stability of the aggregates due to the change in the counterion. The dissociated dodecyl sulfate in ChDS was excluded from the center of mass and moment of inertia calculations that will be discussed on this and on the next section.

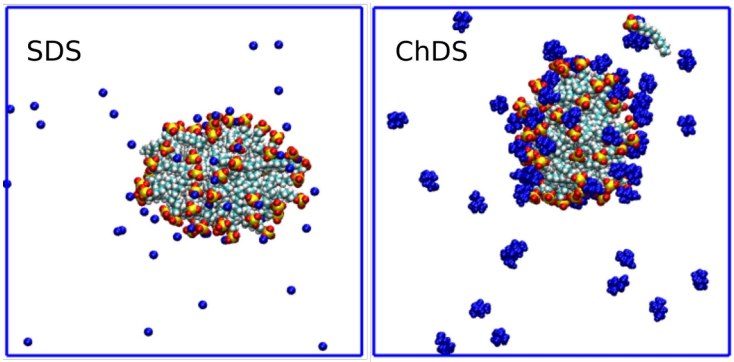

Figure 1 – Graphical representations of the simulation boxes showing the micelles with their respective counter-ions. Counterions are shown in blue while surfactant atoms are represented with the following colors: Hydrogen (gray), Carbon (cyan), Oxygen (red) and Sulfur (yellow). Water molecules were hidden for better visualization.

Both micelles displayed nearly spherical shapes, as can be seen by the graphical representations (Figure 1) and also by the average values of the moments of inertia and radius of gyration across the three mutually orthogonal principal axes (Table 1) computed for the micelle only as well as for the micelle with the adsorbed counterions. The components I_j of the moment of inertia were computed by Equation 1, where m_i is the mass of each atom and r_{ij} is the distance between the atom and the reference axis that passes through the structure center of mass. The principal axes are computed at every frame with the one that results in the smallest possible momentum being the axis number 1. For I_3 is used the axis that is perpendicular to I_1 and which results in the largest momentum. The component I_2 is computed along the remaining mutually orthogonal axis and results in an intermediate value. The components of the radius of gyration were computed based on the components of inertial moment across the principal axis using Equation 2, where M is the total mass of the structure (the micelle or the micelle with adsorbed counterions).

$$I_j = \sum_i m_i r_{ij}^2 \quad \text{(Equation 1)}$$

$$R_{g,j} = \sqrt{\frac{I_j}{M}} \quad \text{(Equation 2)}$$

For a perfect sphere, the three components of the moment of inertia would be identical. Since this is not the case, both micelles present an ellipsoidal component. This can

be quantified by the calculation of eccentricity e (Equation 3, where I_{aver} is the average between the three components of inertia moment). A value of e=0 would imply a perfect sphere while $0 < e < 1$ describes an ellipsoid. The value larger but still close to zero indicates that, although the micelles are not spheres, the deviations from spherical shape are small (Table 1). The comparison between the two systems also showed that the change of the counterion between sodium and choline also didn't induce any significant change in the shape of the micelle at least under the assumption that the aggregation number remains nearly the same.

$$e = 1 - \frac{I_1}{I_{aver}} \quad \text{(Equation 3)}$$

The inclusion of the adsorbed counterions in the calculation of the moment of inertia and radius of gyration results in a systematic increase of those values, as expected since more particles were included in the calculation. The increases are larger for ChDS than for SDS since the choline cation is bulkier and heavier than the sodium and the association degree is larger for ChDS (see discussion next). The eccentricity, however, remains essentially unchanged as well as the conclusions regarding the micelle shape.

Table 1 – Moment of inertia components I_i along principal axes, the components of the radius of gyration R_{gi} along principal axis and the eccentricity of the micelles in both ChDS and SDS systems. Analyses were performed two times for each system, one considering only the surfactant while the other considered the surfactant with the counterions in the first shell.

System	ChDS		SDS	
Species used in the calculation	Surfactant only	Surfactant + adsorbed counterions	Surfactant only	Surfactant + adsorbed counterions
I_1 (10^4 au nm^2)	2.55 ± 0.11	3.38 ± 0.17	2.54 ± 0.12	2.63 ± 0.12
I_2 (10^4 au nm^2)	2.92 ± 0.12	3.87 ± 0.19	2.96 ± 0.14	3.05 ± 0.15
I_3 (10^4 au nm^2)	3.19 ± 0.14	4.21 ± 0.21	3.22 ± 0.15	3.34 ± 0.18
R_{g1} (nm)	1.27 ± 0.03	1.33 ± 0.03	1.26 ± 0.03	1.27 ± 0.03
R_{g2} (nm)	1.35 ± 0.03	1.43 ± 0.03	1.36 ± 0.03	1.37 ± 0.03
R_{g3} (nm)	1.42 ± 0.03	1.49 ± 0.03	1.42 ± 0.03	1.43 ± 0.03
Eccentricity	0.12 ± 0.03	0.12 ± 0.06	0.13 ± 0.04	0.12 ± 0.06

Besides not resulting in any significant change in the shape of the micelle, the substitution of the sodium by the choline produces remarkable effects on the ionization degree, which have consequences for the electrostatic potential and intermicellar interactions. As noticed by the structures in Figure 1, the choline cation has a stronger tendency to be adsorbed at the micelle surface than the sodium counterion. This can described on a quantitative basis by computing the association number of the counterions in both systems (Figure 2). The cation association degree is defined as the number of different surfactant heads in contact with a given cation at a given time. A surfactant head group was considered in contact with the cation if the distance between any oxygen atom of the surfactant is at a distance smaller than 0.32 nm of the sodium atom in SDS or smaller than 0.4 nm of any choline hydrogen atom in ChDS. We chose the oxygen atoms of dodecyl sulfate heads and hydrogen atoms for choline cations to define the contacts since those atoms are the exposed ones in both species and the distances were defined based on the positions of the minima of radial distribution function between those atoms (Figures S1 and S2 in Supporting Information). The counterion association is a dynamic and reversible process, hence the fluctuations displayed in the time evolution in Figure 2 even after a running average was performed in the curves. Since those curves only displayed fluctuations around the average, without systematic trends, we can conclude that the counterions achieve an equilibrium state fairly quickly in the simulations starting from the pre-assembled micelle.

Comparing the two systems, while in the SDS the majority of Na^+ ions show an association number of zero (black curves in Figure 2), meaning they are not associated with the micelle, for the choline cations in ChDS about half of the cations are associated with at least one surfactant head. The ionization degree can be computed directly from this data by dividing the average number of cations with association number of zero by the total number of cations, resulting in 0.83 ± 0.05 for SDS and 0.48 ± 0.04 for ChDS. Wei *et al.* also reported the ionization degree for the ChDS and found the value of 0.16 ± 0.05,[19] significantly smaller than ours. However, their simulations were performed at a concentration *ca* 2.5 times higher and an increase in concentration will always decrease the ionization degree. Also, our simulations were performed at a higher temperature, which can also contribute to a higher ionization assuming that the dissociated state is entropically favorable.

In addition to the high ionization degree, when a sodium is associated with the micelle, it is more likely to interact with a single head group and rarely with two, while for choline cation the simultaneous interaction with two surfactant heads is slightly more likely than the interaction with a single head and even interactions with three and four head groups are common for this cation. This can be attributed both to the larger volume of the choline when compared to the sodium cation, which enables the former to interact with more heads at the same time without the need to bring them too close to each other, and to the presence of OH group in choline in addition to the ammonium group which enables the formation of hydrogen bonds with the surfactant as a secondary form of interaction that is not present in SDS. Another factor that contributes to the larger adsorption of the choline cations at the micelle surface is the higher hydrophobic nature of this cation when compared to sodium, which makes the loss of some first shell water molecules when get into contact with the surfactant easier than for the sodium cation. Figure 3 highlighted the structure of the surfactant and water molecules around choline cations at the micelle surface with coordination numbers of 1, 2 and 3.

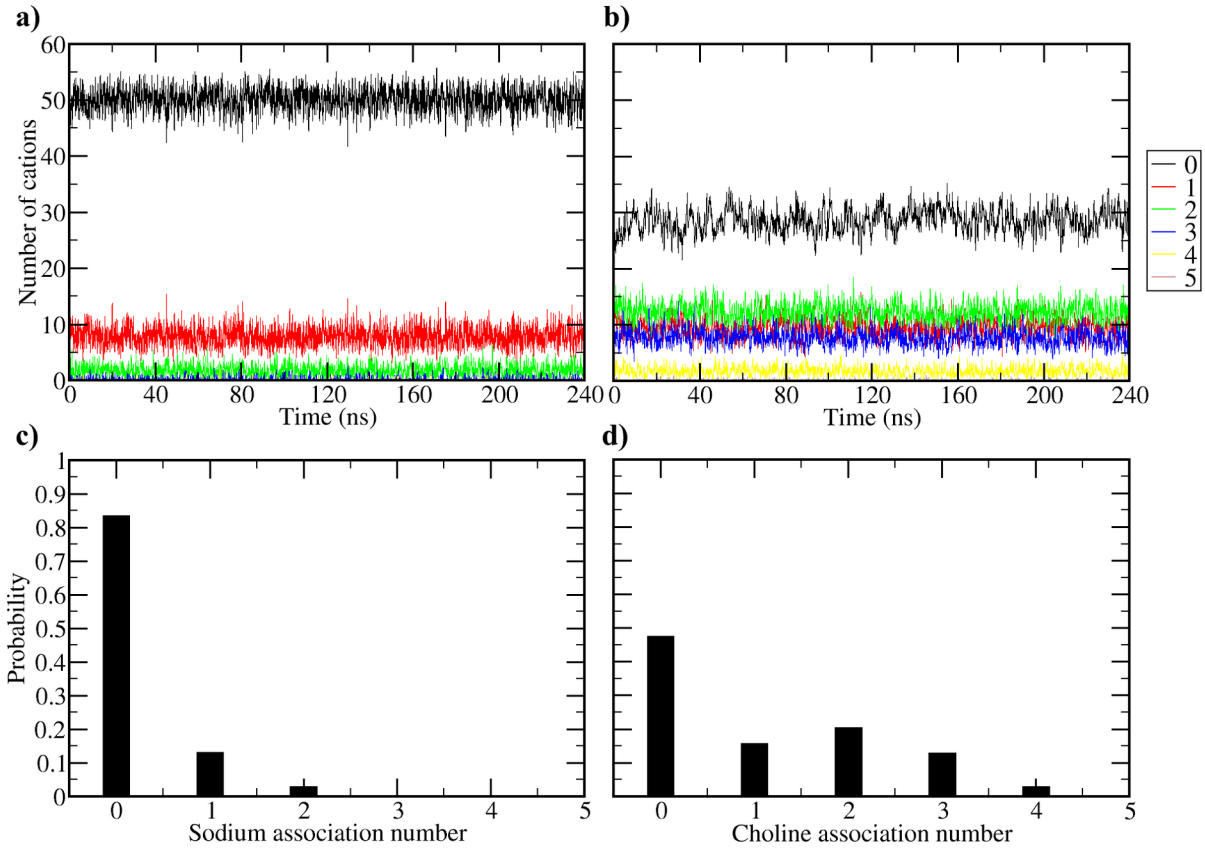

Figure 2 – **a** and **b)** Number of cations with each association number with surfactant head groups along the simulations of SDS (a) and ChDS (b). A running average was performed at each 10 points for each curve for better visualization. **c** and **d)** Histograms with the probability of each coordination number for sodium (c) and choline (d).

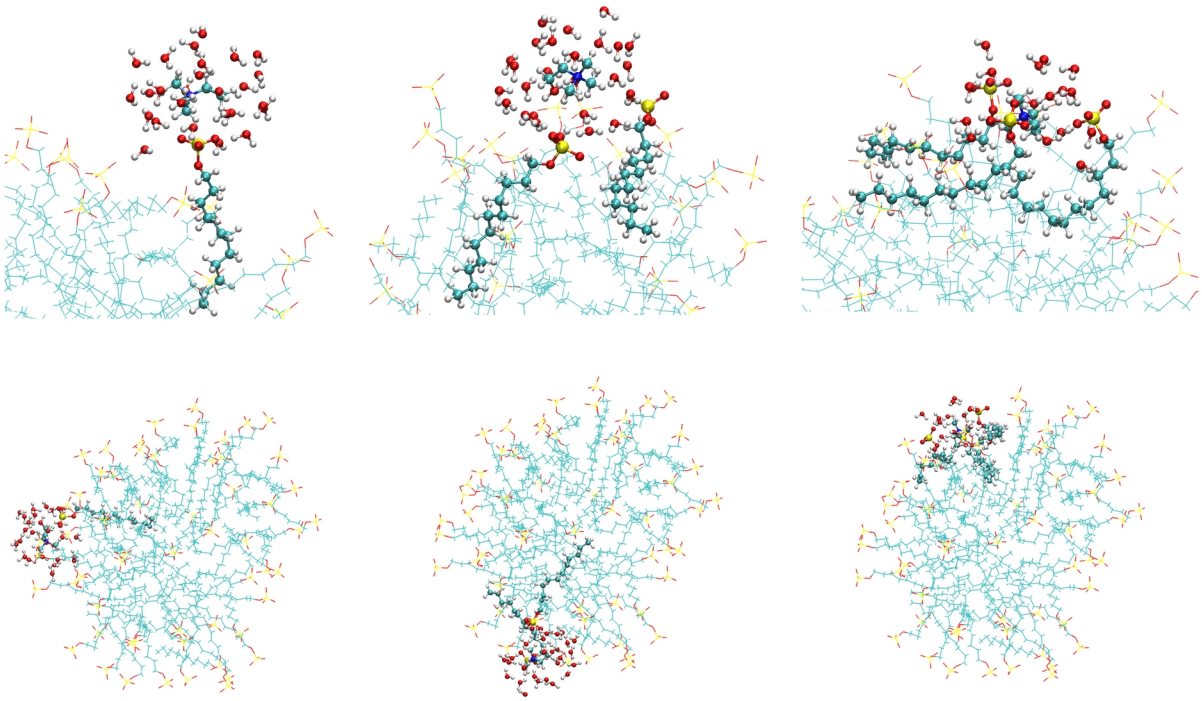

Figure 3 – Organization of surfactant and water molecules in the first coordination shell of adsorbed choline cations with coordination number of (from left to right) 1, 2 and 3. The selected choline cation and species in contact with them are displayed as ball and stick models while other dodecyl sulfate anions are represented with lines. At the top a zoom close to the choline is displayed while at the bottom the whole micelle is shown with the same molecules highlighted. Atoms are represented with the following colors: Hydrogen (gray), Carbon (cyan), Oxygen (red) and Sulfur (yellow).

The stronger association and the bulkier nature of the choline when compared to sodium affects the area of the micelle that is exposed to the solvent (Table 2). The total area of the micelle (first column of Table 2) is essentially the same in both systems. However, when subtracting the surface area of the surfactant that is shielded by the contact with a counterion (second column), the area that is really accessible to water molecules in ChDS micelle is significantly smaller than in the SDS micelle. It is important to notice that in both systems there is still some contact between water molecules and the hydrophobic tails of the surfactant. Due to the electrostatic repulsion between surfactant heads, the micelle structure close to the interface is relatively open (see structures in Figure 3). Also, the stronger interaction between the head group and water results in the formation of coordination shells that can propagate up to the second or the third carbon in the aliphatic chain. This results in

water penetration in distances smaller than the maximum of the radial distribution function of surfactant head groups (Figure 4) and this results in a considerable hydration of the first 2 or 3 carbon atoms as noticed for other surfactants in previous works.[47] However, no water penetration is noticed in distances smaller than 1.2 nm, implying that the micelle core is dry as expected.

Table. 2 – Solvent accessible surface area of the SDS and ChDS micelles, including the shield of Na^+ and choline counterions. In order to guarantee an easier comparison, only the portion of the trajectories prior to the surfactant dissociation were used for ChDS.

System	Total surfactant exposed area (nm^2)	Surfactant area excluding the counter-ions bonded (nm^2)	Counterion shield (nm^2)
SDS	109	101	8
ChDS	109	79	30

Despite the large association of the choline cation over the micelle surface, which leads to a significant reduction in the hydration of the surfactant heads and a drop of *ca.* 9% in the number of hydrogen bonds the surfactant can make with water, the formation of hydrogen bonds between the choline cation itself and the surfactant are not so common (Table 3). From an average number of 31 choline cations at the micelle surface, only 8 are donating hydrogen bonds to the surfactant. For instance, for the choline cations highlighted in the structure of Figure 3, only on the structure in the right the choline OH group is establishing a hydrogen bond with the surfactant, in the others this group is only involved in hydrogen bonds with water. This shows that, despite choline can form hydrogen bonds with the surfactant due to the OH group, the most important interaction is still the ionic interaction with the ammonium portion of the cation. The dominance of the ionic interaction also results in the broader radial distribution function curve for the oxygen of the choline around the micelle center of mass (red dashed curve in Figure 4) than for the nitrogen atom (green dashed curve in Figure 4). The choline oxygen atom can be closer to the micelle center of mass than the nitrogen atom due to the bulk CH_3 groups around the latter. This does not indicate a preference of the O to point toward the micelle core since it also presents a higher g(r) than the N around 2.5 nm and the distance between their maxima is nearly the N-C bond length, meaning CH_3 bonded to N can penetrate as deeper as the OH group.

The number of hydrogen bonds between choline and water is slightly above 1.5 per choline cation, but the hydrogen bonds between choline cations are very rare. In simulations of concentrated solutions of choline salts with oxyanions, hydrogen bonds between choline cations were also very rare, on the other hand, the number of hydrogen bonds between choline cations and both the acetate and dihydrogenophosphate cations was significant.[41] However, the comparison should be made with caution since the differences in the concentration can result in a high impact on the number of cation-anion interactions in general and in the number of hydrogen bonds in particular. In a solution with a high concentration of choline cations, as would be the case in a deep eutectic solvent or in mixtures of deep eutectic solvents with water, the interaction between the surfactant and choline will be amplified and a greater shielding effect will be observed in comparison with the results discussed here where choline is present only as the surfactant counterion.

Table. 3 – Average number and standard deviation of hydrogen bonds along the SDS and ChDS simulations.

System	Hydrogen bond	Average number and stardard deviation
SDS	surfactant-water	402 ± 9
ChDS	surfactant-water	367 ± 10
	surfactant-choline	8 ± 3
	choline-water	95 ± 5
	choline-choline	0.1 ± 0.4

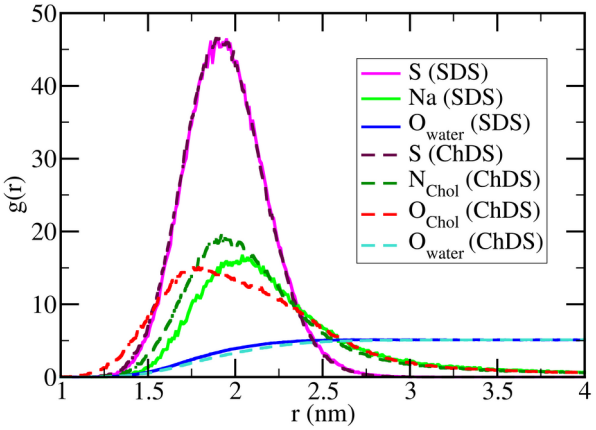

Figure 4 - Radial distribution function between the micelle center of mass and selected atoms, with solid lines for SDS and dashed lines for ChDS. The radial distribution function of the water oxygen was scaled by a factor of 5 for better visualization.

3.2. Electrostatic potential

Charged surfaces in aqueous solutions induce the formation of the electric double layer, which consists of a distribution of counterions between the surface and the solution.[1,2,21] This can be seen by the radial distribution of the counterions (green curves in Figure 4), which displays in both SDS and ChDS systems a maximum nearly in the same distance from the micelle center as the surfactant head (Figure 4) and then decreases smoothly as getting farther from the aggregate. As discussed in the previous section, the choline displays a stronger adsorption at the micelle surface which results in a higher maximum at the micelle surface and a faster decrease toward the bulk solution in comparison to sodium cation. The counterions and water molecules cannot penetrate inside the hydrophobic core of the micelle, as seen in the radial distribution functions of both going to zero for $r < 1.0$ nm in both systems. However, the ammonium group of the choline cation can penetrate deeper inside the polar region of the micelle than the sodium cation. This effect cannot be attributed to a difference in the micelle shape and size, as the distribution of the surfactant head remains essentially the same in both systems and the parameters that describe them are very similar (Table 1), but instead is a result of the smaller charge density and a higher hydrophobic character of the quaternary ammonium group in comparison to the sodium cation.

It is interesting to compare these results with the ones described by Hantal *et al*[8] for alkali metal cations: while they found an increase in the Helmholtz layer thickness with the increase of the cation radius, in our work the opposite trend was found, showing that specific interactions can also play a role in addition to the variation of the ionic radius. Also, the geometry of the surface was different as their study was performed for a flat surfactant monolayer instead of a micelle and this affect counterion adsorption as well.[20]

Since each atom in the system has a fixed partial charge in the simulation (Tables S1 to S4 in the Supporting Information file), by the distributions of each atom type in relation to the micelle center of mass, the average charge density at each spherical shell of radius *r* around the micelle center of mass can be computed and split into contributions arising from each molecule or ion in the system (Figure 5). As expected, in both systems the surfactant contributes to a strongly negative charge density at the micelle surface (pink curves in Figure 5). However, close to the center of the micelle, there is a region of positive charge density inside the hydrophobic region, where the only species present are the CH_3 and CH_2 groups of the surfactant tail. This phenomenon was already discussed in our previous works[20,21] and occurs in both flat surfactant monolayers and spherical micelles and results from the preferential orientation of the surfactant alkyl tails. Although considered as apolar since the dipole moments of neighbors CH_2 tend to cancel each other, at least in *anti* conformation, the carbon atoms and hydrogen atoms of the tail have negative and positive partial charges, respectively. In an idealized micelle structure, with all tails in *anti* conformation and pointing radially from the center of the micelle, closer to its center there will be a region with only H atoms of the CH_3 groups, leading to an excess of positive charge at the center of the cluster. Although the charge is small, the volume of the spherical shell when *r* approaches zero also becomes small, rendering a large charge density. Of course, moving a little outward from the center of the micelle in this idealized structure we would find the carbon atoms of CH_3 group with a negative charge density which neutralizes the positive charge density of the hydrogen atoms. Realistic micelles are more disordered than this idealized view with straight alkyl chains perfectly oriented, however, it is still more likely to find the positively charged hydrogen atoms close to the center of the micelle than the negatively charged carbon atoms, hence there is a region with a positive charge density close to the center but this is quickly neutralized by the charge of carbon atoms as moving farther from the center. Since this region suffers no influence of the counterions, the results for small *r* are essentially the same

for SDS and ChDS. However, at the micelle surface and beyond the counterion starts to display remarkable effects.

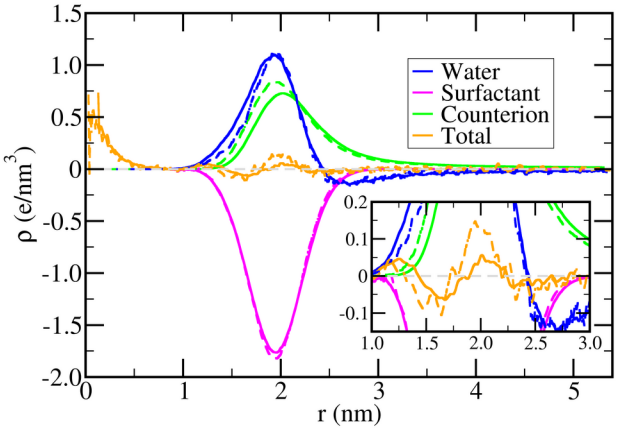

Figure 5 - Charge density of SDS components represented by solid lines and ChDS components represented by dashed lines and the total charge density in the respective systems. The inset zooms over the total charge density curve close to the micelle surface.

The radial distribution function of the surfactant heads is essentially unaffected by the exchange of the counterion between sodium and choline, hence, the charge density due to the surfactant head is nearly the same in both systems. However, as choline penetrates a little deeper inside the micelle than sodium, the positive charge density arising from the counterion (green curves in Figure 5) starts to grow at smaller distances in ChDS than in the SDS system. Also, as the adsorption of the choline cation is stronger, the maximum of the counterion charge density curve is also higher for ChDS, indicating that choline is more efficient in neutralizing the negative charge of the surfactant head group. Notice, however, that neither counterion neutralizes completely the negative charge of the surfactant in the interfacial region, with water molecules also playing an important role in neutralizing it. Besides the fact water molecules have no net charge, they can assume a preferential orientation with the positively charged hydrogen atoms pointing toward the negative surface of the micelle, resulting in regions with positive charge density from water due to an excess of hydrogen atoms (blue curves in Figure 5).

It is interesting to notice that in the ChDS system the contribution of water molecules to the charge density (dashed blue curve) starts only at a greater distance from the micelle

center of mass than in the SDS system (solid blue curve). This has two causes. First, the water penetration in the polar region of the micelle is smaller in the ChDS than in SDS as can be noticed by the radial distribution function curves (cyan and blue curves in Figure 4), which is naturally due to the larger association of the choline with head groups when compared with sodium cations. Second, since the cations neutralize more efficiently the surfactant charge in ChDS than in SDS system, the driving force to orient water molecules around the micelle becomes smaller. This can be quantified by computing the average value of the cosine of the angle θ defined between the vector connecting the micelle center of mass to the oxygen of water molecule and its dipole moment vector μ, as shown at the top of Figure 6. If the oxygen atom is pointing toward the micelle, $\theta < 90^0$ and cos(θ) will be positive. On the other hand, if the hydrogen atoms are the ones pointing toward the micelle, $\theta > 90^0$ and cos(θ) will be negative. The average orientation at a distance *r* was computed including every water molecule whose oxygen atom was located between *r* and *r* + 0.1 nm from the micelle center of mass. The average value of cos(θ) for both systems is negative, indicating a preferential orientation with the positive portion of the molecules pointing toward the negative micelle, as expected. Those curves present global minima closer to the micelle surface and tend smoothly to zero as moving some nanometers far from the micelle surface. Comparing the two systems, the average value of cos(θ) is more negative for SDS at every distance, confirming that on this system there is a stronger orientation effect over water molecules than in the ChDS system.

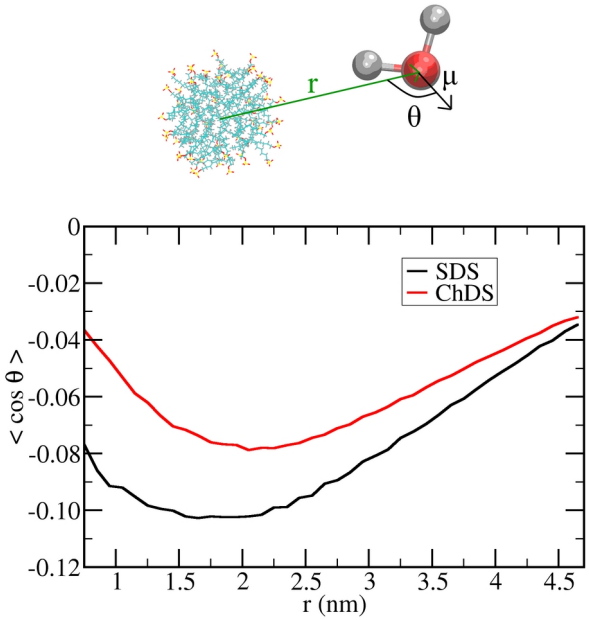

Figure 6 – Average orientation of water molecules at different distances from the micelle center of mass. Top: Definition of θ as the angle defined by the vector *r* between the micelle center of mass and water oxygen atom and the dipole moment μ of the molecule. Bottom: average value of the cosine of the angle θ at each spherical shell of radius *r* around micelle center of mass.

The total charge density is given by the sum of the contributions of each component of the system (orange curves in Figure 5) and, despite the individual components resulting in very large charge densities, they cancel each other in a large extension and the total charge density at the micelle surface is about 20 times smaller than the individual components. This results in a poor noise/signal ratio for the total charge density computed, since small uncertainties on the individual components are of a similar order of magnitude as the total charge density, an issue that was also noticed in our previous works.[20,21] Even with the relatively high noise, a complex pattern can be noticed with alternated regions with positive and negative charge densities. Water can penetrate more deeply than both counterions and surfactant heads, and close to 1.0 nm the positive contribution from water is the dominant, but is quickly surpassed by the negative charge density of the surfactant heads leading to a negatively charged region around r=1.5 nm. Beyond that distance, the counterion contribution increases faster and water contribution is also high, leading to a region with a positive charge

density near r=2.0 nm, which is more positive in ChDS than in SDS due to the stronger adsorption of the choline cation. Close to r=2.3 nm, the water contribution changes signal and becomes negative while there is still some significant probability of finding surfactant head groups, which results in another negatively charged region.

As discussed in the previous section, although not exactly spherical, our micelles are very close to the spherical shape. Hence, we can assume that the charge distribution presents on average a spherical symmetry to compute the electrostatic potential ψ. If the average charge density depends only on the distance *r* from the center of the aggregate, the average potential at a given distance *r* depends only on the total amount of charge Q(*r*) inside the sphere or radius *r*, a well-known result from the application of Gauss law in problems with spherical symmetry (Equation 4, in which Q(*r*) is the accumulated charge inside a sphere of radius *r* centered on the micelle center of mass and ε_0 is the vacuum permittivity). The accumulated charge Q(*r*) can be computed from the integral of the charge density ρ(*r*) (Figure 5) in spherical coordinates (Equation 5). Equations 4 and 5 are valid not only for the total potential, but also for the contributions arising from the surfactant, the counterion and the solvent charge densities. Even if the deviations from the spherical symmetry were considerable, this approach can still be used to compute a time-averaged potential assuming that the medium is isotropic and that the cluster can rotate and the average of all possible orientations describes a sphere.

$$\psi(r) = \frac{Q(r)}{4\pi\varepsilon_0 r} \quad \text{(Equation 4)}$$

$$Q(r) = 2\pi \int_0^r \rho(r) r^2 dr \quad \text{(Equation 5)}$$

The electrostatic potential and the contribution of each species are given in Figure 7 with solid lines for SDS and dashed lines for ChDS while the respective accumulated charge Q(r) profiles are shown in Figure S3 of the Supporting information file. As in the case of the charge density (Figure 5), the individual contributions for the electrostatic potential are huge, of the order of tens of volts, but the opposite contributions cancel each other to a large extent, resulting in a total potential *ca.* 20 times smaller than the individual contributions. As in the case of the charge density, this results in relatively large noise, but for the potential this is less severe since the integral performed (Equations 4 and 5) reduces the effect of random noise.

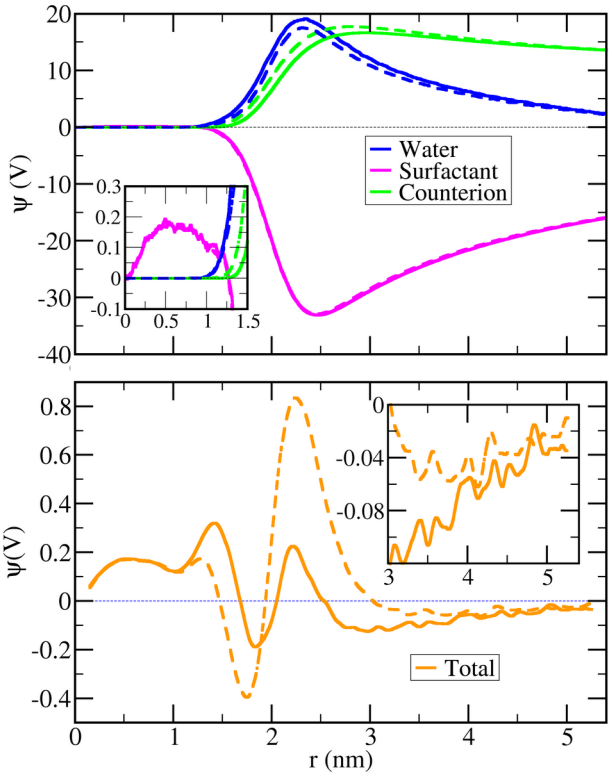

Figure 7 – Top: Contributions of each component for the electrostatic potential. Bottom: Resulting electrostatic potential where a running average at each 20 points was used to reduce the noise. Results for the SDS system are given as solid lines while results for ChDS system are given by dashed lines. Insets zoom over the region inside the micelle for components and on the solution outside the micelle for the total potential.

Despite the charge density being large in the center of the micelles (Figure 5) due to the aliphatic hydrogen atoms, the accumulated charge tends to zero as r→0 since the volume by which the charge density is multiplied ($2\pi r^2 dr$ factor in Equation 5) tends to zero (Figure S3). Hence, the electrostatic potential tends to zero close to the center of the micelle (Figure 7). Still, there is a potential variation inside the hydrophobic core which can be important for the orientation of solutes incorporated into the micelle and for chemical reactions inside micelles.

As in the charge density, the effect of the counterions over the electrostatic potential only appears for r>1.0 nm. The profile for SDS and ChDS are qualitatively similar, with a positive region due to the sharper increase of water positive charge density that happens a

little bit before the strong negative charge density due to the sulfate headgroups which leads to a region with a negative potential. The negative minimum at this region happens in a larger *r* for SDS than for ChDS due to the stronger orientation and large water penetration in the former which leads also to a stronger contribution of water molecules to the potential (blue curves in Figure 7). Around r=2.3 nm, there is another region of positive potential due to a large increase in the positive contribution of the counterions while the contribution of water also remains high. This region of positive potential at the micelle interface can be important to enable the adsorption of species with the same charge of the surfactant at the micelle surface. Due to the stronger association of the choline cation, this positive peak is much more intense for ChDS than for SDS. Since the water contribution arises from a dipole orientation instead of a net charge, its contribution decreases faster than the contributions of ionic species after the micelle surface. This leads to a negative potential region after the micelle surface which remains for long distances from the micelle surface. This region is described as a diffuse double layer in analytical models.[2,48] Moving away from the micelle, the surfactant contribution goes toward zero proportionally to Q_{tot}/r, where Q_{tot} is the total charge of the micelle, if the dissociation of surfactant ions can be neglected. The counterion contribution, on the other hand, decreases slower since, despite *r* increasing, the total charge Q(*r*) due to the counterion also increases since, differently from the surfactant, there is a significant concentration of counterions far from the micelle surface. Comparing both systems in this diffuse layer region, the potential of ChDS is less negative than the potential of SDS, which is again due to the stronger adsorption of the choline cations over the micelle surface. In the description of the Stern model of the electric double layer, the large adsorption means more counterions in the Helmholtz layer, which neutralizes partially the charge of the surface and, as a consequence, reduces the strength of the electrostatic potential produced by the structure in the solution and the double layer thickness.

Despite the complex behavior of the electrostatic potential close to the micelle surface, the potential far from the surface can be described by Equation 6, which is essentially a screened coulomb potential for a spherical surface, where κ is the reciprocal of Debye double layer thickness and *A* is a constant of proportionality.[2,48] Both A and κ can be estimated by fitting Equation 6 to the electrostatic potential curves for large *r* (Figure 8). Only values of r > 3.3 nm were considered for the fitting since at this distance the radial distribution function for surfactant head group atoms goes to zero in the SDS system (in

ChDS it doesn't go to zero outside the micelle due to the dissociation of one surfactant ion). The obtained value of A of -1.46 V.nm for SDS is significantly more negative than the value of -0.37 V.nm for ChDS, indicating that a negative particle would be subject to a stronger repulsion close to the SDS micelle than close to the ChDS micelle, which is due to the larger counterion adsorption in the latter which neutralizes better the micelle charge. Interestingly, the κ for SDS is 0.43 nm^{-1} while for ChDS is only 0.20 nm^{-1}. The larger value for κ implies in a faster decrease in the absolute value of the electrostatic potential for SDS than for ChDS far from the micelle surface. The larger counterion adsorption in the ChDS system results in a small number of ions in the diffuse portion of the electric double layer, which results in a smaller electrostatic screening far from the micelle. This would be described as a reduction of the ionic strength which implies smaller κ values in analytical models for the electric double layer. All in all, the greater counterion adsorption in the ChDS micelle results in weaker negative potential close to the surface, but also in a smaller electrostatic screening in the solution.

$$\psi(r) = A\frac{\exp(-\kappa r)}{r} \quad \text{(Equation 6)}$$

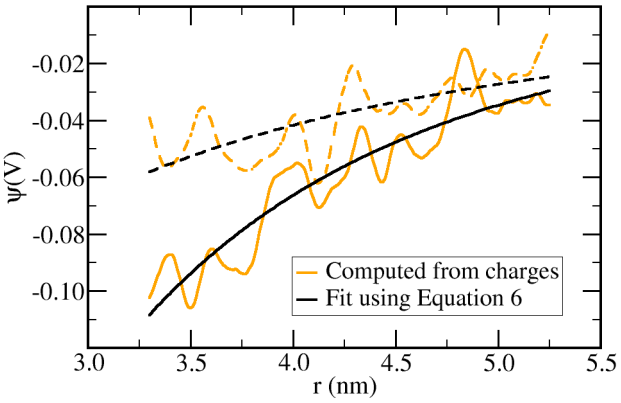

Figure 8 – Long range behavior of the total electrostatic potential computed from charge distributions (Equations 4 and 5) and fit using Equation 6. Results for SDS are given as solid lines while results for ChDS are given by dashed lines. Fitting parameters: A(SDS) = -1.46 V.nm, A(ChDS) = -0.37 V.nm, κ(SDS) = 0.43 nm^{-1}, κ(ChDS) = 0.20 nm^{-1}. Correlation coefficient: 0.93 for SDS and 0.77 for ChDS.

4. Conclusions

The adsorption over the dodecyl sulfate micelle surface is stronger for choline than for the sodium cation, which, along with the fact that the choline is bulkier, reduces the surfactant exposed area to water. This can contribute to the larger micelles formed in choline-based deep eutectic solvents and their mixtures with water when compared to the micelles in pure water both by leading to a further entropy gain when the hydrophobic tails are hindered from the solvent inside the cluster as well as by reducing the effective repulsion between the surfactant charged heads since each choline cation can efficiently coordinate with several sulfate head groups simultaneously.

Regarding the electrostatic potential, even being an anionic micelle, complex patterns were observed, with alternating regions of positive and negative potential at the micelle/water interface. This results from the different intensities of the contributions of the surfactant, the counterion, and the solvent and the fact that each one starts to increase and decrease at different distances from the micelle center of mass. A balance is noticed between the roles of counterions and water molecules in neutralizing the negative charges from the surfactant: When the counterion adsorption is stronger, the reorientation of water molecules occurs to a smaller extent and the contribution of the solvent to the resulting electrostatic potential is smaller, while the opposite scenario occurs if the adsorption is weaker. The long-range behavior of the potential is also affected by the choice of the counterion, with the larger counterion association in ChDS rendering a less negative potential than in SDS, which can also help to explain the formation of larger anionic micelles in choline-based deep eutectic solvents since the choline adsorption reduces the long-range repulsion between micelles, enabling them to get closer to merge into larger clusters.

Although no change in the micellar shape was induced in our simulations by the substitution of the sodium with the choline cation, this may be due to the presence of a single pre-assembled micelle in our study, which restrained it to the maximum coordination number of 60. Also, the ionic concentration in deep eutectic solvents and their mixtures are larger than observed here by the counterion exchange, not to mention the presence of other molecules like urea or glycerol. Further studies need to be performed to understand how the driving forces for micellar aggregation change in those solvents, but the differences in the

interaction of the cations choline and sodium with the surfactant and the effects over the electrostatic potential will certainly play an important role.

Acknowledgments

We acknowledge the financial support from FAPESP (Grant Numbers 2022/15862-7 and 2023/09350-6) and the "Laboratório Nacional de Computação Científica (LNCC/MCTI, Brazil)" for the use of the supercomputer SDumont (https://sdumont.lncc.br).

1 Tanford C. “The hydrophobic effect: Formation of micelles and biological membranes” John Wiley & Sons, New York,1973.
2 Israelachvili J. N. “*Intermolecular and Surface Forces”*, 3rd ed.; Elsevier Academic Press, San Diego, 2011.
3 Shaban S. M., Kang J., Kim D.-H. (2020) Surfactants: Recent advances and their applications, *Composites Communications* **22**: 100537.
4 Holmberg K. (2004) “Surfactant-templated nanomaterials synthesis” *J. Colloid Interf. Sci.* **274**, 355-364.
5 de Moura A. F., Bernardino K., Dalmaschio C. J., Leite E. R., Kotov N. A. (2015) “Thermodynamic insights into the self-assembly of capped nanoparticles using molecular dynamic simulations” *Phys. Chem. Chem. Phys.* **17**: 3820-3831.
6 Bernardino K., de Moura A. F. (2013) “Aggregation Thermodynamics of Sodium Octanoate Micelles Studied by Means of Molecular Dynamics Simulations” *J. Phys. Chem. B* **117**, 24, 7324–7334.
7 Liu G, Zhang H, Liu G, Yuan S, Liu C (2016) “Tetraalkylammonium interactions with dodecyl sulfate micelles: a molecular dynamics study” *Phys. Chem. Chem. Phys.* **18**: 878-885.
8 Hantal G., Pártay L.B., Varga I., Jedlovszky P., Gilányi T. (2007) “Counterion and Surface Density Dependence of the Adsorption Layer of Ionic Surfactants at the Vapor−Aqueous Solution Interface: A Computer Simulation Study.” *J. Phys. Chem. B* **111**: 1769–1774.
9 Rakitin A. R., Pack G. R. (2004). “Molecular Dynamics Simulations of Ionic Interactions with Dodecyl Sulfate Micelles.” *J. Phys. Chem. B* **108**: 2712–2716.
10 De Moura A. F., Freitas, L. C. G.. (2004). “Molecular Dynamics simulation of the sodium octanoate micelle in aqueous solution: comparison of force field parameters and molecular topology effects on the micellar structure.” *Braz. J. Phys.,* **34**, 64–72.
11 Tang X., Koenig P. H., Larson R. G. (2014) “Molecular Dynamics Simulations of Sodium Dodecyl Sulfate Micelles in Water—The Effect of the Force Field” *J. Phys. Chem. B* **118**: 3864–3880
12 Cunha R.D.; Ferreira L.J.; Orestes, E.; Coutinho-Neto M.D.; de Almeida J.M.; Carvalho R.M.; Maciel C.D.; Curutchet C.; Homem-de-Mello P. (2022) “Naphthenic Acids Aggregation: The Role of Salinity.” *Computation* **10**: 170.
13 Poghosyan A.H., Arsenyan L.H., Shahinyan A.A. (2015) “Shape of Long Chain Alkyl Sulfonate Micelle upon Salt Addition: a Molecular Dynamics Study.” *J. Surfact. Deterg.* **18**, 755–760.
14 Volkov N. A., Tuzov N. V., Shchekin A. K. (2016) “Molecular dynamics study of salt influence on transport and structural properties of SDS micellar solutions” *Fluid Ph. Equilib.* **424**: 114-121.
15 Sammalkorpi M., Karttunen M., Haataja M. (2009). “Ionic Surfactant Aggregates in Saline Solutions: Sodium Dodecyl Sulfate (SDS) in the Presence of Excess Sodium Chloride (NaCl) or Calcium Chloride (CaCl2).” *J. Phys. Chem. B* **113**: 5863–5870.
16 Zana R. (2004) “Partial Phase Behavior and Micellar Properties of Tetrabutylammonium Salts of Fatty Acids: Unusual Solubility in Water and Formation of Unexpectedly Small Micelles” *Langmuir* **20**: 5666–5668.
17 Chowdhury M. R., Moshikur R. M., Wakabayashi R., Tahara Y., Kamiya N., Moniruzzaman M., Goto M. (2019) “*In vivo* biocompatibility, pharmacokinetics, antitumor efficacy, and hypersensitivity evaluation of ionic liquid-mediated paclitaxel formulations” *Int. J. Pharm.* **565**: 219–226.
18 Zeisel S. H., da Costa K. A. (2009) “Choline: an essential nutrient for public health” *Nutr. Rev.* **67**: 615–623.
19 Wei Y., Wang H., Liua G., Wang Z., Yuan S. (2016) “A molecular dynamics study on two promising green surfactant micelles of choline dodecyl sulfate and laurate” *RSC Adv.* **6**: 84090–84097.
20 Bernardino K., de Moura A. F. (2015) “Surface Electrostatic Potential and Water Orientation in the presence of Sodium Octanoate Dilute Monolayers Studied by Means of Molecular Dynamics Simulations” *Langmuir* **31**: 10995−11004.
21 Bernardino K., de Moura A. F. (2019) “Electrostatic potential and counterion partition between flat and spherical interfaces” *J. Chem. Phys.* **150**: 074704
22 Tamucci J. D., Alder N. N., May E. R (2023). “Peptide Power: Mechanistic Insights into the Effect of Mitochondria-Targeted Tetrapeptides on Membrane Electrostatics from Molecular Simulations” *Mol. Pharmaceutics* **20**: 6114–6129.
23 Gurtovenko, A. A., Vattulainen, I. (2008) “Membrane Potential and Electrostatics of Phospholipid Bilayers with Asymmetric Transmembrane Distribution of Anionic Lipids” *J. Phys. Chem. B* **112**: 4629–4634.

24 Gurtovenko A. A., Vattulainen, I. (2009) “Calculation of the electrostatic potential of lipid bilayers from molecular dynamics simulations: Methodological issues”. *The Journal of Chemical Physics* **130**: 215107.
25 Smith E. L., Abbott A. P., Ryder K. S. (2014) “Deep Eutectic Solvents (DESs) and Their Applications” *Chem. Rev.* **114**, 11060–11082.
26 Coutinho J. A., Pinho S. P. (2017) “Special issue on deep eutectic solvents: a foreword” *Fluid Ph. Equilib.* **448**, 1.
27 Abbott A. P., Capper G., Davies D. L., Rasheed R. K., Tambyrajah V. (2003) "Novel solvent properties of choline chloride/urea mixtures". *Chem. Commun.* **1**, 70–71.
28 Shekaari H., Zafarani-Moattar M. T., Shayanfar A., Mokhtarpour M. (2018) “Effect of choline chloride/ethylene glycol or glycerol as deep eutectic solvents on the solubility and thermodynamic properties of acetaminophen.” *J. Mol. Liquids.* **249**, 1222-1235.
29 Sanchez-Fernandez A., Edler K. J., Arnold T., Heenan R. K., Porcar L., Terrill N. J., Terry A. E., Jackson A. J. (2016) “Micelle structure in a deep eutectic solvent: a small-angle scattering study” *Phys. Chem. Chem. Phys*. **18**, 14063-14073.
30 Arnold T., Jackson A. J., Sanchez-Fernandez A., Magnone D., Terry A. E., Edler K. J. (2015) “Surfactant Behavior of Sodium Dodecylsulfate in Deep Eutectic Solvent Choline Chloride/Urea” *Langmuir* **31**, 12894−12902.
31 Banjere R. M., Banjere M. K., Behera K., Pandey S., Ghosh K. K. (2020) “Micellization behavior of conventional cationic surfactants within glycerol-based deep eutetic solvent” *ACS Omega* **5**, 19350-19362.
32 Martínez L., Andrade R., Birgin E. G., Martínez, J. M. (2009) “Packmol: A package for building initial configurations for molecular dynamics simulations.” *J. Comput. Chem.* **30:** 2157-2164.
33 Berendsen H. J. C., van der Spoel D., van Drunen R. (1995) “GROMACS: A message-passing parallel molecular dynamics implementation,” *Comp. Phys. Comm.* **91**, 43–56.
34 Abraham M.J., Murtola T., Schulz R., Páll S., Smith J. C., Hess B., Lindahl E. (2015) “GROMACS: High performance molecular simulations through multi-level parallelism from laptops to supercomputers,” *Software X* **1**, 19–25.
35 Bussi G., Donadio D., Parrinello M. (2007) “Canonical sampling through velocity rescaling ” *J. Chem. Phys.* **126**: 014101.
36 Agieienko V., Buchner R. (2019) “Densities, Viscosities, and Electrical Conductivities of Pure Anhydrous Reline and Its Mixtures with Water in the Temperature Range (293.15 to 338.15) K” *J. Chem. Eng. Data* **64**: 4763–4774.
37 Berendsen H. J. C., Postma J. P. M. DiNola A., Haak J. R. (1984) “Molecular dynamics with coupling to an external bath.” *J. Chem. Phys.* **81**: 3684−3690.
38 Jorgensen W. L., Maxwell D. S., Tirado-Rives J. (1996) “Development and testing of the OPLS all-atom force field on conformational energetics and properties of organic liquids.” *J. Am. Chem. Soc.* **118**: 11225−11236.
39 Granovsky A. A. “Firefly (formerly PC http://classic.chem.msu.su/gran/firefly/index.html. 2009. GAMESS) homepage”.
40 Schmidt M. W., Baldridge K. K., Boatz J. A., Elbert S. T., Gordon M. S., Jensen J. H.; Koseki S., Matsunaga N., Nguyen, K. A., Su S.; Windus T. L., Dupuis M., Montgomery J. A. (1993) “General atomic and molecular electronic structure system”. *J. of Comput. Chem.* **14**: 1347-1363.
41 de Souza Í. F. T., Paschoal V. H., Bernardino K., Lima T. A., Daemen L. L., Ribeiro M. C. C. (2021) “Vibrational spectroscopy and molecular dynamics simulation of choline oxyanions salts” *J. of Mol. Liq.* **340**: 117100.
42 Neese F. (2012) “The ORCA program system” *Wiley Interd. Rev.-Comput. Mol, Science* **2**: 73–78.
43 Berendsen H. J. C.; Postma J. P. M.; van Gusteren W. F.; Hermans J. *In Intermolecular Forces*; Pullman, B., Ed.; Reidel: Dordrecht, 1981.
44 Åqvist J. (1990) “Ion-water interaction potentials derived from free energy perturbation simulations.” *J. Phys. Chem.* **94**: 8021−8024.
45 Essmann U., Perera L., Berkowitz M. L., Darden T., Lee H., Pedersen L. G. (1995) “A smooth particle mesh Ewald method,” *J. Chem. Phys.* **103**: 8577–8593 .

46 Humphrey W., Dalke A., Schulten K. (1996) “VMD - Visual molecular dynamics,” *J. Mol. Graphics* **14.1**, 33–38.
47 de Moura A. F., Bernardino K., de Oliveira O. V., Freitas L. C. G (2011) “Solvation of Sodium Octanoate Micelles in Concentrated Urea Solution Studied by Means of Molecular Dynamics Simulations” *J. Phys. Chem. B* **115**, 14582–14590.
48 Dill K. A., Bromberg S. Molecular Driving Forces : Statistical Thermodynamics in Chemistry and Biology. New York, Garland Science, 2002.

Supporting Information file for

Counterion adsorption and electrostatic potential in sodium and choline dodecyl sulfate micelles - a molecular dynamics simulation study

Rafaela Eliasquevici[1], *Kalil Bernardino*[1]*

* kalilb@ufscar.br

1. Laboratório de Química Computacional, Departamento de Química, Universidade Federal de São Carlos, Rod. Washington Luiz S/n, 13565-905 São Carlos, Brazil

Contents:

1. Tables including the partial charges and Lennard-Jones parameters for all species present in the simulations and for dihedral angles of the choline cation which were reparametrized.
2. Radial distribution function between selected atoms of the surfactant and the counter ions used to define the cut off distance employed in the determination of association numbers.
3. Accumulated charge from each chemical species around the micelle center of mass (defined in Equation 4 of the main text and used to compute the electrostatic potential as in Equation 3).

Table S1 – Partial charges and Lennard-Jones parameters for dodecyl sulfate.

Atom	q (e)	ε (kJ/mol)	σ (nm)
S	1.284	1.046000	0.355
O (bonded only to S)	-0.654	0.711280	0.296
O (C-O-S)	-0.459	0.711280	0.300
C (from CH_2 bonded to head)	0.017	0.276144	0.350
C (from other CH_2)	-0.120	0.276144	0.350
C (from terminal CH_3)	-0.180	0.276144	0.350
H	0.060	0.125520	0.250

Table S2 – Partial charges and Lennard-Jones parameters for choline.

Atom	q (e)	ε (kJ/mol)	σ (nm)
O	-0.683	0.711280	0.312
N	-0.008	0.711280	0.325
C (CH_3 bonded to N)	0.090	0.276144	0.350
C (CH_2 bonded to N)	0.150	0.276144	0.350
C (CH_2 bonded to O)	0.145	0.276144	0.350
H (bonded to C)	0.060	0.125520	0.250
H (bonded to O)	0.418	0.000000	0.000

Table S3 – Partial charges and Lennard-Jones parameters for sodium (Åqvist parameters).

Atom	q (e)	ε (kJ/mol)	σ (nm)
Na	1.000	0.011598	0.333045

Table S4 – Partial charges and Lennard-Jones parameters for water (SPC model).

Atom	q (e)	ε (kJ/mol)	σ (nm)
O	-0.820	0.650194	0.316557
H	0.410	0.000000	0.000000

Table S5 – Parameters for Ryckaert-Bellemans function used to describe dihedral angles of the choline cation that were reparametrized from the original OPLS-AA force field (values in kJ/mol).

Dihedral	C_0	C_1	C_2	C_3	C_4	C_5
N-C-C-O	223.27236776	-2.43302684	2.02582148	0.76256715	0.61590863	0.38680925
C-C-O-H	83.57190464	1.84400893	-3.76911786	-4.22542943	6.64022733	3.14606529

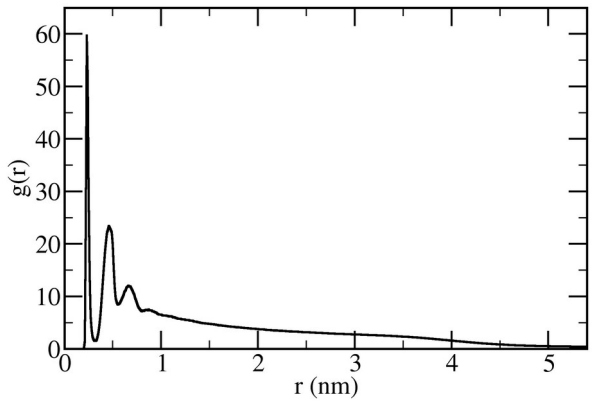

Figure S1 – Radial distribution function between oxygen atoms of the surfactant and sodium counterions in SDS simulation.

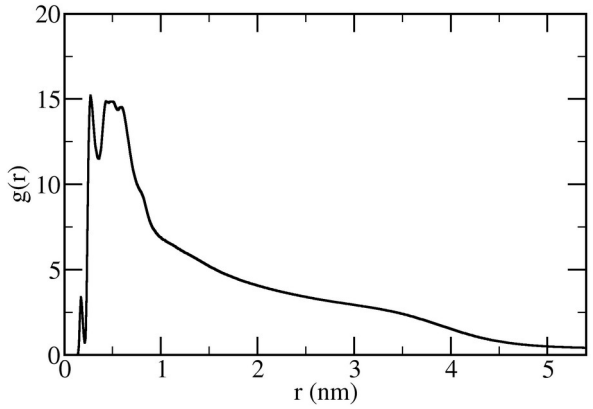

Figure S2 – Radial distribution function between oxygen atoms of the surfactant and hydrogen atoms of the choline cation in ChDS simulation. The first small and sharp peak occurs at 0.28 nm and corresponds to the hydrogen of choline OH group making a hydrogen bond with the surfactant. The criteria for the aggregation, however, was based on the second minimum at *ca.* 0.4 nm which also include hydrogen groups of CH_3 and CH_2 groups in contact with the surfactant head.

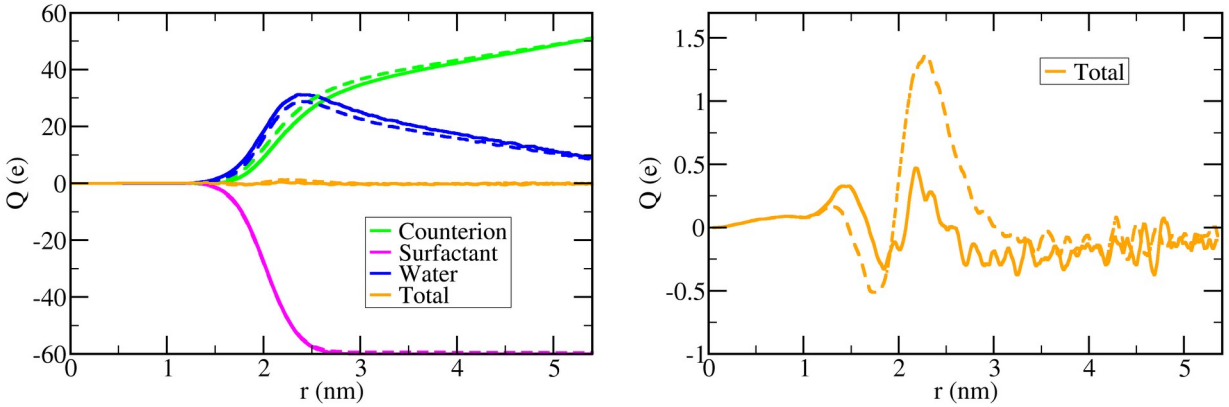

Figure S3 – Time-averaged value of the accumulated charge at each distance *r* from the micelle center of mass with results from SDS system represented as solid lines and for ChDS system as dashed lines. Left: Components from each species, Right: Zoom at the the total accumulated charge. A running average was performed at every 10-points of the total accumulated charge curves for better visualization.